

Photocatalytic degradation of trace hexane in the gas phase with and without ozone addition: kinetic study

Pengyi Zhang*, Juan Liu

Department of Environmental Science and Engineering, Tsinghua University, Beijing 100084, China

Received 30 December 2003; received in revised form 30 March 2004; accepted 18 May 2004

Available online 20 June 2004

Abstract

The degradations of trace hexane in the gas phase by O_3/UV , TiO_2/UV and $O_3/TiO_2/UV$ were studied. The effects of the flow rate, inlet concentration of hexane, water vapor concentration and ozone dosage on the conversion of hexane in the three processes were investigated, respectively. The experimental results showed that the addition of ozone significantly increase photocatalytic degradation of hexane. The reaction rates of hexane by O_3/UV and $O_3/TiO_2/UV$ increased linearly with an increase of ozone addition, which increased faster in O_3/UV than in $O_3/TiO_2/UV$. L–H bimolecular model was successfully used to correlate photocatalytic reaction rate data under various hexane and water vapor concentrations. A new model combining L–H model and ozone photolysis was developed to correlate reaction rate data of hexane in $O_3/TiO_2/UV$.

© 2004 Elsevier B.V. All rights reserved.

Keywords: Photocatalysis; Ozonation; Hexane; Titanium dioxide; Ozone; Indoor air

1. Introduction

The pollution of indoor volatile organic compounds (VOCs) has been increasingly concerned in recent years. The heterogeneous photocatalysis mostly based on titanium dioxide is considered as one of the most promising methods to decompose indoor VOCs. Photocatalysis has an advantage over activated carbon adsorption in that it can decompose VOCs completely rather than transfer to another phase. In the past few decades, researchers have investigated photocatalytic degradation of a variety of gaseous VOCs including alkanes [1–3], alkenes [1,4], alcohols [5], aldehydes and ketones [6–8], chlorinated hydrocarbons [5,9], aromatics [1,10–12] and others [13,14].

However it has been reported that TiO_2 photocatalyst may be deactivated after a period of use. For example, in the study of photocatalytic oxidation of heteroatom organics, Peral and Ollis [15,16] found irreversible catalyst deactivation in the case of decamethyltetrasiloxane, pyrrole and indole. Larson and Falconer [17] reported that dichloroacetyl chloride (DCAC) formed and strongly adsorbed to TiO_2 during trichloroethylene (TCE) photo-oxidation, which re-

sultantly reduced TCE adsorption. Alberici et al. [18] also detected several by-products like phosgene, DCAC and trichloroacetyl chloride during photocatalytic oxidation of tetrachloroethylene, TCE, chloroform and dichloromethane using on-line mass spectrometry and MS/MS method. Similarly benzoic acid accumulated on catalyst and catalyst deactivation occurred during photocatalytic oxidation of toluene [12,19–21]. The buildup of *o*-toluic acid on the catalyst surface may also be responsible for the apparent loss of catalyst activity during the photocatalytic oxidation of dilute *o*-xylene in air [22].

To avoid deactivation of photocatalyst and increase the photocatalytic degradation rate of contaminants, many efforts have been made. For example, it was demonstrated that photocatalytic oxidation rate of aqueous contaminants and TOC reduction rate were greatly increased with addition of oxidants such as ozone [23,24], hydrogen peroxide and persulfate [25–27]. Shen and Ku [28] studied the decomposition of gas-phase TCE by the TiO_2/UV process in the presence of ozone. They found that the addition of ozone into the $UV/TiO_2/TCE$ system with 254 or 365 nm UV lamp reduced the conversion of TCE, which possibly because excessive ozone molecules could scavenge hydroxyl radicals produced from the excitation of TiO_2 by UV radiation. One of the authors [29] compared the degradation of trace benzene (1.0–20 ppm) in the gas phase by O_3/UV , TiO_2/UV and

* Corresponding author. Tel.: +86-10-62784527;

fax: +86-10-62794006.

E-mail address: zpy@mail.tsinghua.edu.cn (P. Zhang).

$O_3/TiO_2/UV$. It was found that the addition of ozone to the photocatalysis process could greatly increase the conversion of toluene. And in particular the deactivation of the photocatalyst at high inlet concentration of toluene was avoided in the presence of ozone. Kim et al. [30] also reported that photocatalytic degradation of benzene and toluene was increased by high voltage discharge, in which ozone was generated.

Hexane is a major indoor and industrial air pollutant, and it was recommended as one of the eight representative indoor VOCs by a proposed ASHRAE test method for determining the effectiveness and capacity of gas-phase air filtration equipment for indoor air applications [31]. The effect of ozone on photocatalytic degradation of alkanes has never been investigated until now. In the present paper, the photocatalytic degradations of hexane with and without ozone were studied, and the effects of flow rate, hexane concentration, humidity and ozone dosage on the decomposition of hexane were examined to find out rate expressions for hexane decomposition by TiO_2/UV and $O_3/TiO_2/UV$.

2. Experimental

2.1. Preparation of supported titanium dioxide

The TiO_2 film coated on the aluminum sheet used in this study was prepared by a modified sol–gel method. Tetrabutylorthotitanate ($Ti(OC_4H_9)_4$, C.P.), acetyl acetone (C_5H_8O , A.R.), deionized water and *n*-propanol (C_3H_8O , A.R.) were mixed with a volumetric ratio of 1:0.3:0.4:7 at room temperature. Nanometer carbon black powder (Degussa Printex L6, the primary particle size 18 nm and BET surface $265\text{ m}^2/\text{g}$) was added in the above sol at the ratio of 1 mL $Ti(OC_4H_9)_4$:2.35 mg carbon black and was mixed uniformly by sonification. The prepared mixture could be stably stored for several months. The polished aluminum sheet was dipped in the mixture and then dried at room temperature before heated at 500°C for 2 h. After the aluminum sheet was dipped and heated seven times (which was previously optimized), a thin TiO_2 photocatalyst film was formed on it. The TiO_2 film was very stable and durable without any loss during experiments.

2.2. Experimental set-up

A schematic diagram of the experimental system for photo-oxidation is shown in Fig. 1. The saturated hexane gas was prepared by passing air through a thermostated saturator containing liquid hexane. The humidified air stream was generated by bubbling air through a thermostated glass bottle containing deionized water. Then the saturated hexane gas was mixed and diluted with humidified air stream in the gas mixer. The obtained hexane gas stream was fed into the photoreactor at flow rates between 5 and $17\text{ L}/\text{min}$, inlet hexane concentrations between 4.94 and $26.9\text{ mg}/\text{m}^3$ and relative humidity (RH) in the range of 12–60%. Feed

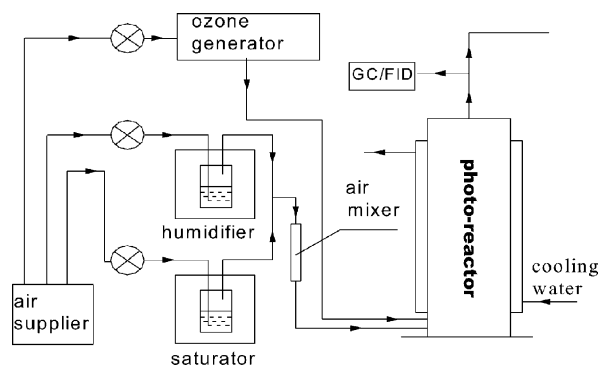


Fig. 1. Schematic diagram of the experimental apparatus.

hexane concentrations and relative humidity were set by varying the ratio of gas flow rates and/or varying the saturator temperature. The ozone air stream ($250\text{ mL}/\text{min}$) from ozone generator was directed into the photoreactor with the nominal production of $15\text{ mg}/\text{h}$. In ozone dosage experiments, another ozone generator (nominal production $100\text{ mg}/\text{h}$) was used, and different ozone outputs were obtained by adjusting voltage of ozone generator.

The cylindrical photoreactor was made of stainless steel with a diameter of 64 mm and a length of 530 mm, with effective volume of 1.44 L. The outside of the photoreactor was a cooling water sleeve to maintain stable reaction temperature (20 – 22°C). Illumination was provided with a 15 W germicidal lamp with maximum light intensity output at 254 nm. The lamp was fixed at the center of the photoreactor without quartz tube protection. The TiO_2 coated aluminum sheet (length 440 mm, height 201 mm and thickness 0.18 mm) closely attached the interior surface of the photoreactor. For O_3/UV process, no catalyst or blank aluminum sheet was used.

2.3. Analyses and procedures

The concentration of hexane was analyzed on-line by a HP5890 II model gas chromatograph with a flame ionization detector (FID). The gas samples were collected periodically using a six-way valve with a gas sampling loop ($500\ \mu\text{L}$) and transferred into a packed column (AT OV 101) with a diameter of 3 mm and a length of 2 m. The gas chromatograph oven temperature maintained constant at 250°C . In this work, no intermediates from the degradation of hexane were identified by the gas chromatograph probably due to its detection limit. The concentrations of ozone in influent and effluent streams were determined by iodometry method. The humidity analyzer was used to monitor relative humidity of the mixed air stream.

When the reactor outlet concentration equaled the reactor inlet concentration, the lamp was turned on. And after the photocatalytic (TiO_2/UV) or photolytic (UV) steady state reached, it was kept lasting for at least 150 min. Then the ozone generator was turned on and ozone was fed

into the photoreactor. The ozone-enhanced photo-oxidation ($\text{O}_3/\text{TiO}_2/\text{UV}$ or O_3/UV) usually reached steady after a few minutes. Similarly it also lasted at least 150 min.

The conversion η (%) and reaction rate (r) of hexane were calculated, respectively, as follows:

$$\eta = \frac{C_{\text{in}} - C_{\text{out}}}{C_{\text{in}}} \times 100\%$$

$$r = (C_{\text{in}} - C_{\text{out}}) \frac{Q}{V}$$

where C_{in} is the inlet concentration, C_{out} the outlet concentration at steady state, Q the flow rate of air stream, and V the volume of photoreactor (1.44 L).

3. Results and discussion

In the blank tests, the photolysis of hexane by 254 nm UV irradiation alone was found to be trivial. The conversions of hexane by ozone alone or combined with TiO_2 in the absence of irradiation were less than 5% under the experimental condition in this study. Thus the contributions by O_3 , O_3/TiO_2 and UV in the processes of TiO_2/UV , O_3/UV and $\text{O}_3/\text{TiO}_2/\text{UV}$ could be neglected.

3.1. Effect of flow rate

Fig. 2 shows the effect of flow rate on the decomposition of hexane at the inlet concentration of 10.10–11.35 mg/m^3 and relative humidity of 35%. It was found that the reaction rate of hexane initially increased with flow rate and reached a plateau when the flow rate was larger than 12 L/min in both TiO_2/UV and $\text{O}_3/\text{TiO}_2/\text{UV}$ processes, while it fluctuated a little with flow rate in the process of O_3/UV . In any case, the reaction rate by $\text{O}_3/\text{TiO}_2/\text{UV}$ was significantly larger than that of TiO_2/UV , and the O_3/UV was much less efficient in decomposing hexane than the former two processes.

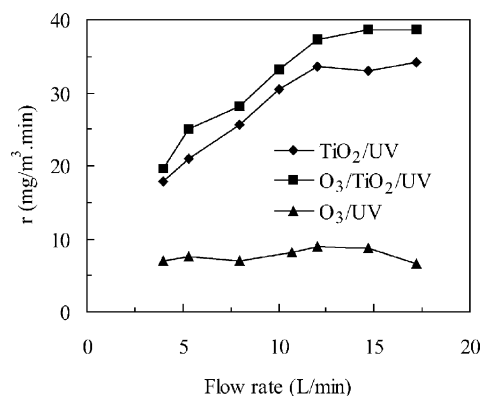


Fig. 2. Effect of flow rate on the reaction rate of hexane by O_3/UV , TiO_2/UV or $\text{O}_3/\text{TiO}_2/\text{UV}$ processes (inlet concentration 10.10–11.35 mg/m^3 , RH 35%).

In heterogeneous photocatalysis, the reaction occurred on the surface was influenced by mass transfer from the gas phase to photocatalyst surface. As seen from Fig. 2, as for TiO_2/UV and ozone-enhanced photocatalysis ($\text{O}_3/\text{TiO}_2/\text{UV}$), the reaction was controlled by the mass transfer at low flow rate, however the mass transfer influence decreased with increase of flow rate and became small when the flow rate was larger than 12 L/min. Similar results were reported by Wang et al. [32] who found the degradation rate of trichloroethylene by TiO_2/UV was no longer influenced by flow rate when the flow rate was larger than 0.3 L/min due to elimination of mass transfer effect. Thus, to obtain accurate data for kinetic analysis, the later experiments were conducted at the flow rate of 12 L/min to eliminate the influence of mass transfer.

Because in the O_3/UV process the reaction happened in the gas phase, its reaction rate was little influenced by the flow rate. However, the ozone concentration in the gas phase decreased a little as the flow rate increased, thus the reaction rate varied with flow rate as seen in Fig. 2.

3.2. Effect of hexane concentration

The effect of inlet concentration of hexane on its conversion is shown in Fig. 3. The results correspond to the flow rate of 12.0 L/min (residence time 7.2 s) and relative humidity of 35%. As seen in Fig. 3, the conversions in all processes including O_3/UV , TiO_2/UV and $\text{O}_3/\text{TiO}_2/\text{UV}$ decreased with increase of inlet concentration of hexane. Hexane degraded by $\text{O}_3/\text{TiO}_2/\text{UV}$ much faster than by TiO_2/UV , which demonstrated the addition of trace ozone (only 15–16 mg/m^3) significantly increased the photocatalytic degradation of hexane. The enhancement of ozone on photocatalysis was mainly due to two reasons [29]: (1) ozone substituted for oxygen as photo-generated electron acceptor; (2) ozone was photolyzed by 254 nm UV light and hydroxyl radical was produced resultantly. However, the conversion by $\text{O}_3/\text{TiO}_2/\text{UV}$ was less than the sum of conversion by TiO_2/UV and O_3/UV . It was because ozone

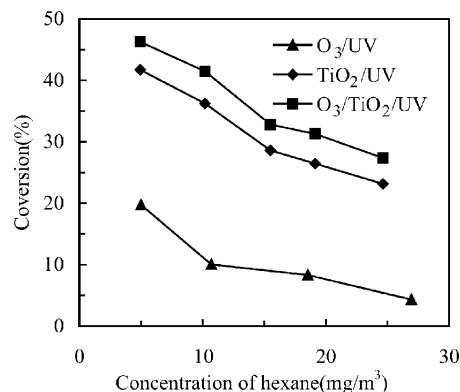


Fig. 3. Effect of inlet concentration on the conversion of hexane by O_3/UV , TiO_2/UV or $\text{O}_3/\text{TiO}_2/\text{UV}$ processes (flow rate 12 L/min, RH 35%).

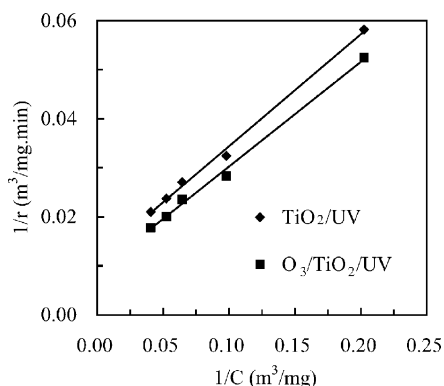


Fig. 4. Linear fitting of the $1/r$ vs. $1/C$ (flow rate 12L/min, RH 35%).

could compete with VOC like hexane to scavenge hydroxyl radicals [33]. Besides, the presence of ozone also attenuated the UV intensity on the photocatalyst because of its high absorption coefficient at 254 nm.

Langmuir–Hinshelwood (L–H) rate expression has been widely used in gas-phase and liquid-phase photocatalysis. If the concentrations of water and oxygen remain constant, this equation can be simplified as follows:

$$r = \frac{kKC}{1 + KC}$$

where r is the reaction rate ($\text{mg}/\text{m}^3 \text{ min}$), C the concentration of hexane (mg/m^3), k the reaction rate constant ($\text{mg}/\text{m}^3 \text{ min}$), and K the adsorption constant (m^3/min). Inverse of the equation gives

$$\frac{1}{r} = \frac{1}{kKC} + \frac{1}{k}$$

If the assumed L–H form is valid, then a plot of $1/r$ versus $1/C$ should be linear. Fig. 4 indicates that the degradations of hexane in both TiO_2/UV and $\text{O}_3/\text{TiO}_2/\text{UV}$ process are in good agreement with L–H model. The experimental data of O_3/UV did not fit the L–H model certainly because it was not a surface reaction. The equations of linear regression for TiO_2/UV and $\text{O}_3/\text{TiO}_2/\text{UV}$ were described, respectively, as follows:

$$\text{TiO}_2/\text{UV} : \quad \frac{1}{r} = 0.2284 \frac{1}{C} + 0.0116,$$

$$R^2 = 0.9966, \quad k = 86.2 \text{ mg}/\text{m}^3 \text{ min}, \quad K = 0.0508 \text{ m}^3/\text{mg},$$

$$\text{O}_3/\text{TiO}_2/\text{UV} : \quad \frac{1}{r} = 0.2134 \frac{1}{C} + 0.089,$$

$$R^2 = 0.9959, \quad k = 112.4 \text{ mg}/\text{m}^3 \text{ min},$$

$$K = 0.0417 \text{ m}^3/\text{mg}$$

Comparing the reaction rate constant (k) and adsorption constant (K) of the above two processes, it was found that though k increased about 30% from 86.2 to 112.4 $\text{mg}/\text{m}^3 \text{ min}$ due to ozone addition, the K decreased from 0.0508 to 0.0417 $\text{m}^3 \text{ mg}^{-1}$ probably due to ozone competitive adsorption with hexane on the photocatalyst surface.

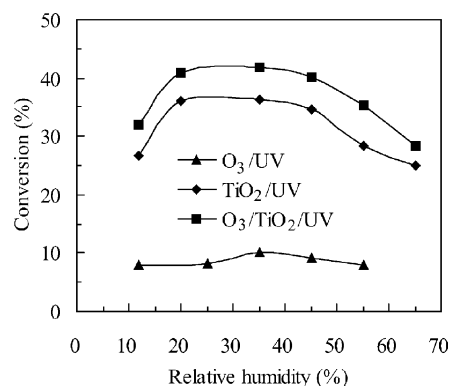


Fig. 5. Effect of relative humidity on the conversion of hexane by TiO_2/UV , O_3/UV or $\text{O}_3/\text{TiO}_2/\text{UV}$ processes (inlet concentration $10.45 \text{ mg}/\text{m}^3$, flow rate 12.0L/min).

3.3. Effect of relative humidity

The effects of relative humidity on the photocatalytic oxidation of VOCs including hexane have been investigated by many authors [1,2,4,10,21,34–36]. In this study, the degradations of hexane at the relative humidity ranging from 12 to 65% (corresponding water concentration ranges from 238 to 7000 mg/m^3) common to indoor air were investigated. The results are shown in Fig. 5. It was found that the O_3/UV process was little affected by the variation of relative humidity. As for the processes of TiO_2/UV and $\text{O}_3/\text{TiO}_2/\text{UV}$, the conversions of hexane initially increased greatly with increase of relative humidity up to 20% and then almost kept stable until 45%, however it significantly decreased when the relative humidity was larger than 45%. It indicated that in photocatalysis or ozone-enhanced photocatalysis a little humidity would improve the decomposition of trace hexane while too much humidity would depress the decomposition. This feature agrees with the results reported in literatures. Martra et al [35] and Augugliaro et al. [36] reported that removing water from the feed would result in deactivation of catalyst, which indicated that the water was necessary to maintain the surface-OH on the TiO_2 for hydroxyl radical production. In the absence of water, the initial reaction rate of toluene [21] and hexane [2] dropped drastically in a limited time. Also other studies [1,10,22,32,34] showed that increase of water concentration increased or decreased the photocatalytic reaction rate, depending on the type and concentration of VOCs. Cao et al. [21] reported the initial reaction rate decreased with an increase of water concentration resulting from competitive adsorption of water with toluene on TiO_2 surface.

3.4. Effect of ozone dosage

Fig. 6 shows the effect of ozone dosage on the reaction rates of hexane conducted at the inlet concentration of $11.45 \text{ mg}/\text{m}^3$ and 12L/min flow rate. It was found that in

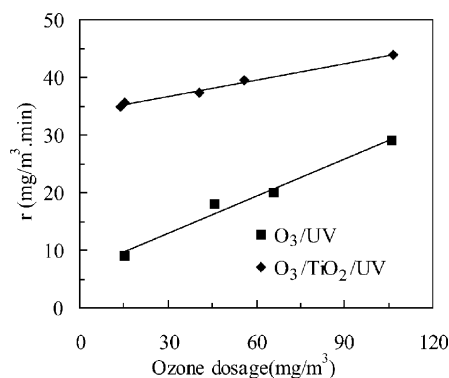


Fig. 6. Effect of the ozone dosage on the reaction rate of hexane by O₃/UV or O₃/TiO₂/UV process (inlet concentration 11.45 mg/m³, flow rate 12.0 L/min, RH 35%).

either O₃/UV or O₃/TiO₂/UV process the reaction rate of hexane increased almost linearly with the ozone concentration ranging from 15.2 to 106 mg/m³. It indicated that the hexane degradation in O₃/UV or O₃/TiO₂/UV process obey the first order with ozone concentration. However the effect of ozone concentration were much more significant in O₃/UV than that in O₃/TiO₂/UV process, the slope in O₃/UV was nearly two times of that in the later. The different effect of ozone in two processes is probably due to the following two reasons. First, as we know, ozone is not only a source but also a scavenger of hydroxyl radical [28,29,33], and ozone also will scavenge O produced by ozone photolysis to form oxygen [23]. Thus at higher ozone dosage, if reactant such as hexane molecules is not enough for reaction with hydroxyl radical or O, the radical will be scavenged by excessive ozone. In comparison with O₃/TiO₂/UV, the reaction rate of O₃/UV is much smaller, the reaction is less limited by deficiency of hexane molecules and thus increase more fast with increase of ozone dosage. Secondly, higher ozone concentration will attenuate the UV irradiation available to the photocatalyst. For example, when ozone concentration is 15.2 mg/m³, it can be calculated that the UV attenuation due to O₃ absorbing is only 4.5%, while it is 27.7% when the ozone concentration is as high as 106 mg/m³. Accordingly the reaction rate contributed by TiO₂ photocatalysis will decrease due to reduction of UV intensity.

3.5. Kinetics of hexane degradation by TiO₂/UV

As described above when the concentrations of water and oxygen remained constant, the hexane degradation by TiO₂/UV was in good agreement with L–H model. When the water or oxygen also varied, L–H bimolecular model was found to provide a good correlation to the photocatalytic reaction rate data [3,32,34]. According to L–H model, the reaction happens between adsorbed reactants. Because different reactants such as hexane and water maybe competitively adsorb on same type of surface site, or adsorb on

different types of surface sites with or without competitiveness, there are three forms of L–H bimolecular model:

$$\text{form 1 : } r = \frac{kK_1C_h}{1 + K_1C_h} \frac{K_2C_w}{1 + K_2C_w},$$

$$\text{form 2 : } r = \frac{kK_1C_hK_2C_w}{(1 + K_1C_h + K_2C_w)^2},$$

$$\text{form 3 : } r = \frac{kK_1C_h}{1 + K_1C_h + K_2C_w} \frac{K_4C_w}{1 + K_3C_h + K_4C_w}$$

where k is the reaction rate constant, K_1 , K_3 the adsorption constant of contaminant such as hexane, K_2 , K_4 the adsorption constant of water, C_h the concentration of contaminant such as hexane, and C_w the water concentration.

Form 1 describes the adsorption of hexane and water on different types of sites without competitive adsorption; form 2 represents adsorption of hexane and water on same type of sites with competitive adsorption; form 3 represents adsorption of hexane and water on different types of sites with competitive adsorption, however water adsorbed on reaction sites of hexane does not involve the reaction, and hexane adsorbed on reaction sites of water does not involve the reaction either. All these forms assume that only hexane and water not reaction products have influences on reaction rate. Using the experimental data presented in Figs. 3 and 5, we performed the simulations for the above three rate expressions. Correlations coefficients for observed versus predicted values of forms 1–3 were 0.8472, 0.9110 and 0.9834, respectively, indicating the suitability of form 3 for the present investigation. The parameters of form 3 were, respectively, $k = 98.2617 \text{ mg m}^{-3} \text{ min}^{-1}$, $K_1 = 0.0634 \text{ m}^3 \text{ mg}^{-1}$, $K_2 = 0.0002 \text{ m}^3 \text{ mg}^{-1}$, $K_3 = 1.2525 \text{ m}^3 \text{ mg}^{-1}$, $K_4 = 0.1376 \text{ m}^3 \text{ mg}^{-1}$. Fig. 7(a) and (b) shows the agreement of experimental data with calculated according to form 3.

According to the model, reaction rate of hexane by TiO₂/UV under various conditions could be predicted. Fig. 8(a) and (b), respectively, shows the reaction rate dependence on hexane and water concentration. As seen in Fig. 8(a), under various relative humidity, reaction rate initially increases greatly to a maximum and then decreases with increase of hexane concentration. In general, low relative humidity is appropriate to reaction of low hexane concentration, while high relative humidity favors reaction of high hexane concentration. As seen in Fig. 8(b), for low hexane concentration like 1 and 5 mg/m³, its reaction rate decreases slowly when the water concentration increases from 865 to 17,291 mg/m³ (corresponding to relative humidity 5–100% at 20 °C), while it sharply increases to reach a maximum and then decreases with increase of water concentration when the hexane concentration is much higher. The higher is the hexane concentration, the higher is relative humidity where the maximum reaction rate reaches.

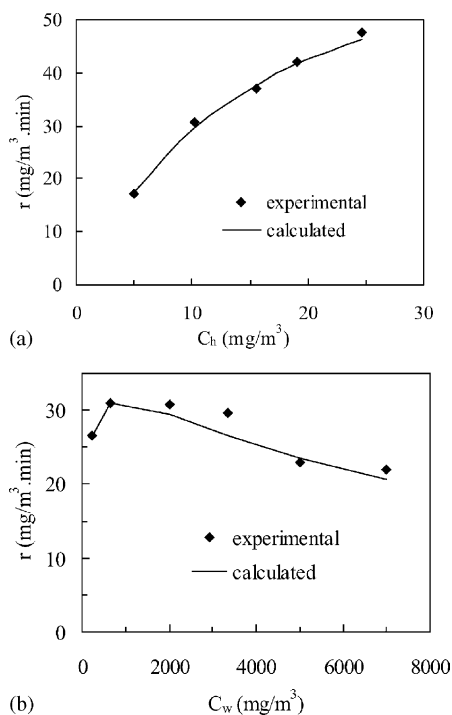


Fig. 7. Fitting of hexane reaction rate by TiO₂/UV with L–H model: (a) hexane concentration; (b) water concentration.

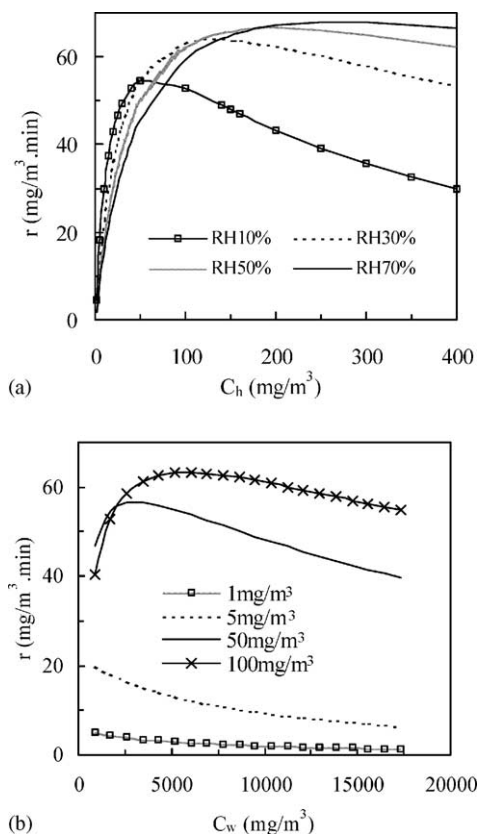
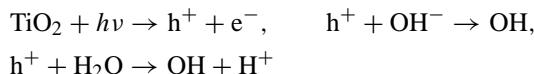


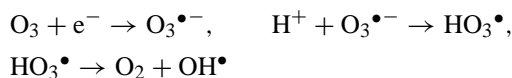
Fig. 8. Predictions of hexane reaction rate by TiO₂/UV depending on (a) hexane and (b) water concentration.

3.6. Kinetics of hexane degradation by O₃/TiO₂/UV

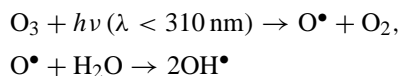
As previously described [29], in the O₃/TiO₂/UV ($\lambda < 310$ nm) process the hydroxyl radical was generated via two pathways: (1) TiO₂ photocatalysis (TiO₂/UV) and (2) ozone photolysis (O₃/UV). In TiO₂ photocatalysis, the generation of hydroxyl radical is described as follows:



In case of ozone addition, ozone substitutes oxygen as acceptor of photo-generated electron and forms hydroxyl radical as follows:



In the ozone photolysis, hydroxyl radical is generated via following reactions:



Thus the degradation of hexane not only happens on the surface of photocatalyst but also occurs in the bulk of gas phase. The surface reaction on photocatalyst can be described with L–H model, and the reaction in the bulk phase can be described by first-order kinetics with ozone concentration if the hexane concentration is excessive. Thus the following reaction rate expression was used to correlate the experimental data in the O₃/TiO₂/UV process:

$$r = \frac{kK_1C_h}{1 + K_1C_h + K_2C_w} \frac{K_4C_w}{1 + K_3C_h + K_4C_w} + k'C_o$$

where k is the surface reaction rate constant, k' the gas phase reaction rate constant, K_1 , K_3 the adsorption constant of contaminant such as hexane, K_2 , K_4 the adsorption constant of water, C_h the concentration of contaminant such as hexane, C_w the water concentration, and C_o the ozone concentration.

We performed the simulation for the above rate expression. Good agreement was obtained as shown in Fig. 9. The parameters of the model were, respectively, $k = 97.7849 \text{ mg m}^{-3} \text{ min}^{-1}$, $k' = 0.104 \text{ mg m}^{-3} \text{ min}^{-1}$, $K_1 = 0.0727 \text{ m}^3 \text{ mg}^{-1}$, $K_2 = 0.0002 \text{ m}^3 \text{ mg}^{-1}$, $K_3 = 0.2716 \text{ m}^3 \text{ mg}^{-1}$, $K_4 = 0.0446 \text{ m}^3 \text{ mg}^{-1}$. According to the above model, the reaction rate (r_1) contributed by surface photocatalysis was calculated at different hexane concentration. The photocatalytic reaction rate (r_2) in TiO₂/UV without ozone addition was also calculated. Comparing r_1 and r_2 , it was found that r_1 was always larger than r_2 as shown in Fig. 10, which clearly indicated that addition of ozone enhanced the photocatalytic degradation of hexane besides the contribution of ozone photolysis.

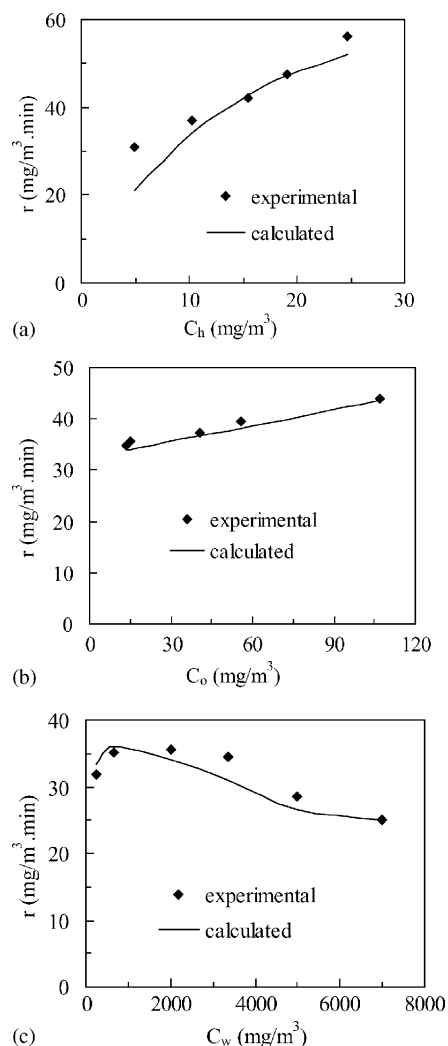


Fig. 9. Fitting of hexane reaction rate by $O_3/TiO_2/UV$ with L–H model: (a) hexane concentration; (b) ozone concentration; (c) water concentration.

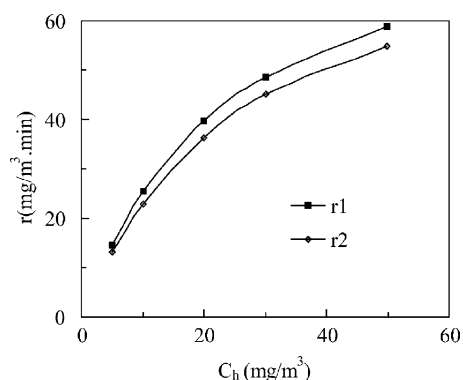


Fig. 10. Comparison of calculated photocatalytic reaction rate in $O_3/TiO_2/UV$ (r_1) and that in TiO_2/UV (r_2) (assuming water concentration is 5187 mg/m³, i.e. RH 30%, flow rate 12.0 L/min).

4. Conclusion

The decomposition of trace hexane in the gas phase by O_3/UV , TiO_2/UV and O_3TiO_2/UV were investigated and compared. The $O_3/TiO_2/UV$ process was the most efficient among these three processes. The conversion rate in all these three processes decreased with increase of inlet concentration of hexane. Relative humidity played a significant role in decomposing hexane in both TiO_2/UV and $O_3/TiO_2/UV$ processes. It was found that a little humidity would improve the decomposition of trace hexane while too high relative humidity (>45%) would depress the decomposition, which resulted from competitive adsorption of water on photocatalyst surface with other reactants. The reaction rate of hexane by O_3/UV and $O_3/TiO_2/UV$ linearly increased with increase of ozone addition. However, it increased more slowly with ozone concentration in $O_3/TiO_2/UV$ than in O_3/UV , which was explained by hexane deficiency and UV attenuation by ozone available to photocatalyst. L–H bimolecular model was successfully used to correlate hexane reaction rate data in TiO_2/UV . Accordingly the reaction rate under various conditions was predicted. A new model combining L–H bimolecular model and ozone photolysis was developed and well correlated hexane reaction rate data in $O_3/TiO_2/UV$. Calculations based on model confirmed that addition of ozone enhanced the photocatalytic reaction besides contribution of ozone photolysis.

Acknowledgements

The authors acknowledge the Natural Science Foundation of China for financial support (grant no. 50178038 and 59908004).

References

- [1] H. Einaga, S. Futamura, T. Ibusuki, *Appl. Catal. B Environ.* 38 (2002) 215.
- [2] X.Y. Deng, Y.H. Yue, Z. Gao, *Appl. Catal. B Environ.* 39 (2002) 135.
- [3] J. Shang, Y.G. Du, Z.L. Xu, *Chemosphere* 46 (2002) 93.
- [4] T.N. Obee, S.O. Hay, *Environ. Sci. Technol.* 31 (1997) 2034.
- [5] R.M. Alberici, W.E. Jardim, *Appl. Catal. B Environ.* 14 (1997) 55.
- [6] J. Peral, D.F. Ollis, *J. Catal.* 136 (1992) 554.
- [7] T. Noguchi, A. Fujishima, *Environ. Sci. Technol.* 32 (1998) 3831.
- [8] A.V. Vorontsov, I.V. Stoyanova, D.V. Kozlov, V.I. Simagina, E.N. Savinov, *J. Catal.* 189 (2000) 360.
- [9] L.A. Dibble, G.B. Raupp, *Catal. Lett.* 4 (1990) 345.
- [10] W.K. Jo, J.H. Park, H.D. Chun, *J. Photochem. Photobiol. A Chem.* 148 (2002) 109.
- [11] C.H. Ao, S.C. Lee, C.L. Mak, L.Y. Chan, *Appl. Catal. B Environ.* 42 (2003) 119.
- [12] S.A. Larson, J.L. Falconer, *Catal. Lett.* 44 (1997) 57.
- [13] G.P. Zanini, G.A. Arguello, *J. Mol. Catal. A Chem.* 159 (2000) 347.
- [14] P. Papaefthimiou, T. Ioannides, X.E. Verykios, *Catal. Today* 54 (1999) 81.
- [15] J. Peral, D.F. Ollis, in: D.F. Ollis, H. Al-Ekabi (Eds.), *Photocatalytic Purification and Treatment of Water and Air*, Elsevier, 1993, p. 741.
- [16] J. Peral, D.F. Ollis, *J. Mol. Catal. A Chem.* 115 (1997) 347.

- [17] S.A. Larson, J.L. Falconer, *Appl. Catal. B Environ.* 4 (1994) 325.
- [18] R.M. Alberici, M.A. Mendes, W.F. Jardim, M.N. Eberlin, *J. Am. Soc. Mass Spectr.* 9 (1998) 1321.
- [19] R. Mendez-Roman, N. Cardona-Martinez, *Catal. Today* 40 (1998) 353.
- [20] Y. Luo, D.F. Ollis, *J. Catal.* 163 (1996) 1.
- [21] L.X. Cao, Z. Gao, S.L. Suib, T.N. Obee, S.O. Hay, J.D. Freihaut, *J. Catal.* 196 (2000) 253.
- [22] M.M. Ameen, G.B. Raupp, *J. Catal.* 184 (1999) 112.
- [23] L. Sanchez, J. Peral, X. Domenech, *Appl. Catal. B Environ.* 19 (1998) 59.
- [24] L.S. Li, W.P. Zhu, P.Y. Zhang, Z.Y. Chen, L. Chen, *Chin. J. Catal.* 24 (2003) 163.
- [25] S. Malato, J. Blanco, C. Richter, B. Braun, M.I. Maldonado, *Appl. Catal. B Environ.* 17 (1998) 347.
- [26] Y.B. Wang, C.S. Hong, *Water Res.* 33 (1999) 2031.
- [27] C.C. Wong, W. Chu, *Environ. Sci. Technol.* 37 (2003) 2310.
- [28] Y.S. Shen, Y. Ku, *Chemosphere* 46 (2002) 101.
- [29] P.Y. Zhang, F.Y. Liang, G. Yu, Q. Chen, W.P. Zhu, *J. Photochem. Photobiol. A Chem.* 156 (2003) 189.
- [30] H.S. Kim, E.A. Lee, J.H. Lee, C.H. Han, J.W. Ha, Y.G. Shul, *Int. J. Photoenergy* 5 (2003) 3.
- [31] D.W. VanOsdell, *ASHRAE Trans.* 100 (1994) 511.
- [32] K.H. Wang, H.H. Tsai, Y.H. Hsieh, *Appl. Catal. B Environ.* 17 (1998) 313.
- [33] P.T. Buckley, J.W. Birks, *Atmos. Environ.* 29 (1995) 2409.
- [34] T.N. Obee, R.T. Brown, *Environ. Sci. Technol.* 29 (1995) 1223.
- [35] G. Martra, S. Coluccia, L. Marchese, V. Augugliaro, V. Loddo, *Catal. Today* 53 (1999) 695.
- [36] V. Augugliaro, S. Coluccia, V. Loddo, L. Marchese, G. Marta, L. Palmisano, M. Schiavello, *Appl. Catal. B Environ.* 20 (1999) 15.